

NASA CR- 66 209

Job 8320

Page i - v

1 - 32

Copy 30 of ()

ANALYTICAL STUDY OF AERODYNAMIC
MEANS OF CONTROLLING SUPERSONIC

INLET FLOW

PART I

TECHNICAL REPORT NO. 495B

by H. Rosenbaum and S.L. Zeiberg

Prepared Under Contract No. NAS1-4387

Prepared for

National Aeronautics and Space Administration

Langley Field, Virginia

Prepared by


General Applied Science Laboratories, Inc.

Merrick and Stewart Avenues

Westbury, Long Island, N.Y.

Distribution of this report is provided in the interest of
information exchange. Responsibility for the contents
resides in the author or organization that prepared it.

Approved by:


Dr. A. Ferri
President

November, 1965

ABSTRACT

39888

There is presented herein a method of achieving a variable geometry inlet without recourse to mechanical devices. The principles of viscous mixing and basic inviscid fluid mechanics are combined by utilizing mass flow injected along the wall of an inlet to provide the desired area changes. For this purpose an analysis for a two-dimensional turbulent jet mixing into an adverse pressure gradient field is presented and numerical solutions for conditions of interest are discussed. It is shown that the basic scheme is a sound one; its drawbacks are discussed and improvements suggested. AUTNPR

TABLE OF CONTENTS

<u>Section</u>	<u>Title</u>	<u>Page No.</u>
	Abstract	ii
	List of Symbols	iv
	List of Figures	v
I	Introduction	1
II	Mixing Analysis	3
III	Calculations	8
	References	14
	Figures	15 - 32

LIST OF SYMBOLS

- a - Slot height or jet radius
- C_p - Turbulent specific heat
- P - External pressure
- T - Stagnation temperature
- u, v - Axial and normal velocity components respectively
- x, y - Axial and normal coordination respectively
- δ - Transformed jet radius
- $\rho\epsilon$ - Eddy viscosity
- η - Transformed normal coordinate
- K - Turbulent thermal conductivity coefficient
- ψ - Stream function
- ρ - Mass density
- σ - $\frac{(\rho\epsilon)C_p}{\kappa}$ = Turbulent Prandtl Number

LIST OF FIGURES

<u>Figure</u>	<u>Description</u>	<u>Page No.</u>
1	Schematic of Mechanically Controlled Variable Contour Inlet	15
2	Schematic of Area Change Necessary For Off-Design Operation	16
3	Schematic of Mixing Controlled Contour	17
4	Schematic of Two-Dimensional Jet	18
5	Schematic of Finite Difference Network	19
6	Effect of Pressure and Mixing on Contours Formed by Jet Spreading	20
7	Contour Formed by Single Slot	21
8	Pressure Gradient for Single Slot	22
9	Contour Formed by Slot Injection	23
10	Pressure Gradient	24
11	Velocity Distribution	25
12	Velocity Distribution	26
13	Schematic of Multi-Slot Injection Scheme	27
14	Contour for Multiple-Slot Injection Scheme	28
15	Pressure Distribution for Multiple-Slot Injection Scheme	29
16	Velocity Before Second Slot Injection	30
17	Velocity Profile Before Third Slot Injection	31
18	Velocity Profile Before Fourth Slot	32

ANALYTICAL STUDY OF AERODYNAMIC MEANS OF
CONTROLLING SUPERSONIC INLET FLOW

PART ONE

I. INTRODUCTION*

The use of variable geometry inlets becomes a necessity when air-breathing propulsion devices are employed at high supersonic Mach numbers. For example, an aircraft cruising at Mach 3 must also possess the off-design capability of efficient Mach 2 operation. To date, all variable geometry inlets are mechanical in operation (see Figure 1). A movable ramp is usually employed to provide the contour change necessary for efficient off-design operation. Such mechanical devices have obvious drawbacks; e.g., their weight and the weight of the equipment needed to move them up and down within the inlet. It is our purpose here to suggest and analyze a possible aerodynamic means of providing variable geometry inlets.

Consider the following situation as depicted schematically in Figure 2; a simple two-dimensional converging channel with the area ratio necessary to provide deceleration from a Mach 2 incoming flow to slightly supersonic conditions at the throat. This, very crudely, is the job an inlet must perform. Now, assume this same inlet has an incoming flow of Mach No. 3; the dotted line represents the additional area reduction necessary to provide near sonic conditions at the throat. Consider next Figure (3), where the lower wall of this inlet is shown with a slot to facilitate tangential mass injection along the inlet length. Let the injected mass flow

* The authors wish to acknowledge the guidance provided by Dr. Antonio Ferri.

be subsonic and have the same static pressure as that of the main stream at the point of injection. The dotted lines represent the streamline emanating from the lip of the slot splitter plate. Since the external flow has an adverse pressure gradient field and the flow from the slot is subsonic, then if the effects of viscous mixing are ignored this streamline will spread and, indeed, grow at an infinite rate as the slot flow is decelerated towards zero velocity (Curve #1 in Figure 3). However, the viscous effects will tend to mix the high stagnation pressure, high velocity outer flow into this subsonic slot flow and energize it. Hence, a streamline configuration, such as Curve 2, in Figure 3, is possible. In fact, by varying the mass flow of the jet it should be possible to obtain, by using the two counteracting effects of inviscid area increase and viscous mixing, any desired streamline pattern. This splitter plate streamline acts as a solid wall to the incoming main flow and thus provides the means for obtaining a variable geometry inlet without recourse to mechanical devices.

The analytical formulation of the scheme discussed above; namely, the tangential slot injection into a turbulent boundary layer is a difficult one. A conceptually simpler analytic model would be that pertaining to a free turbulent jet. This would amount to ignoring the effects of shear at the wall, however, it would retain the essential dynamic features of this scheme, namely the counteracting effects of inviscid area spreading and viscous mixing of the high and low energy streams. Such an analysis is developed in the next section and is applied to problems of physical interest.

II. MIXING ANALYSIS

Consider the mixing of a two-dimensional turbulent jet into a moving stream with an arbitrary pressure gradient (Figure 4). If standard boundary layer techniques are assumed to apply here, the conservation equations are:

1) Continuity

$$\frac{\partial}{\partial x} (\rho u) + \frac{\partial}{\partial y} (\rho v) = 0 \quad (1)$$

2) Momentum

$$\rho u \frac{\partial u}{\partial x} + \rho v \frac{\partial u}{\partial y} = - \frac{dp}{dx} + \frac{\partial}{\partial y} \left[(\rho \epsilon) \frac{\partial u}{\partial y} \right] \quad (2)$$

3) Energy

$$c_p \rho u \frac{\partial T}{\partial x} + c_p \rho v \frac{\partial T}{\partial y} = u \frac{dp}{dx} + (\rho \epsilon) \left(\frac{\partial u}{\partial y} \right)^2 + \frac{\partial}{\partial y} \left[\frac{c_p}{\sigma} (\rho \epsilon) \frac{\partial T}{\partial y} \right] \quad (3)$$

4) State

$$p = \rho R T \quad (4)$$

where:

- T = stagnation temperature
- $\rho \epsilon$ = eddy viscosity
- u, v = axial and normal velocity components respectively
- σ = turbulent Prandtl Number = $\frac{(\rho \epsilon) c_p}{K}$
- K, c_p = turbulent conductivity and specific heats respectively
- p = p(x) = external pressure

The boundary and initial conditions are:

$$x = 0 \quad u = u(y); \quad T = T(y)$$

$$y = 0 \quad \frac{\partial u}{\partial y} = \frac{\partial T}{\partial y} = 0$$

$$y = \pm \infty \quad u = u_e(x); \quad T = T_e(x)$$

It is convenient for the numerical procedure which follows to compute flow properties as functions of the stream function ψ ; thus, a transformation of independent variables $(x, y) \rightarrow (x, \psi)$ is defined as:

$$\frac{\partial \psi}{\partial y} = \rho u$$

(5)

$$\frac{\partial \psi}{\partial x} = -\rho v$$

The transformation (5) identically satisfies the continuity Equation, Equation (1); the momentum and energy equations, Equations (2) and (3), become respectively:

$$\frac{\partial u}{\partial x} = \frac{1}{\rho u} \frac{dp}{dx} + \frac{\partial}{\partial \psi} \left[\rho u (\rho \epsilon) \frac{\partial u}{\partial \psi} \right] \quad (6)$$

$$c_p \frac{\partial T}{\partial x} = \frac{1}{\rho} \frac{dp}{dx} + \frac{\partial}{\partial \psi} \left[\frac{c_p}{\sigma} \rho u (\rho \epsilon) \frac{\partial T}{\partial \psi} \right] + \rho u (\rho \epsilon) \left(\frac{\partial u}{\partial \psi} \right)^2 \quad (7)$$

Equations (5), (6), and (7), form a set of parabolic partial differential equations for which an explicit finite difference integration will be employed, following the analysis of Reference (1). Referring to Figure (5), if $F(x, \psi)$ is any dependent variable, then at any generic point denoted for brevity by n, m , the partial

derivative in the axial direction may be approximated by a backward difference as:

$$\left(\frac{\partial F}{\partial x}\right)_{n,m} = \frac{F_{n,m} - F_{n-1,m}}{\Delta x} + O(\Delta x) \quad (8)$$

The partial derivative in the ψ direction is approximated by the central difference as:

$$\left(\frac{\partial F}{\partial \psi}\right)_{n-1,m} = \frac{F_{n-1,m+1} - F_{n-1,m-1}}{2\Delta\psi} + O((\Delta\psi)^2) \quad (9)$$

and the second derivative operator becomes:

$$\frac{\partial}{\partial \psi} \left[a \frac{\partial F}{\partial \psi} \right]_{n-1,m} = \left[a_{n-1,m+\frac{1}{2}} (F_{n-1,m+1} - F_{n-1,m}) - a_{n-1,m-\frac{1}{2}} (F_{n-1,m} - F_{n-1,m-1}) \right] \left[\Delta\psi^2 \right]^{-1} + O(\Delta\psi^2) \quad (10)$$

where:

$$a_{n-1,m \pm \frac{1}{2}} = \frac{a_{n-1,m} + a_{n-1,m \pm 1}}{2} \quad (11)$$

Use of the difference approximations, Equations 8-11, transforms the partial differential equations into the following set of linear algebraic equations:

$$u_{n,m} = - \frac{\Delta x}{(\rho u)_{n-1,m}} \left(\frac{dp}{dx} \right)_n + \frac{\Delta x}{(\Delta\psi)^2} \left\{ a_{n-1,m+\frac{1}{2}} u_{n-1,m+1} - \left[a_{n-1,m+\frac{1}{2}} + a_{n-1,m-\frac{1}{2}} \right] u_{n-1,m} + a_{n-1,m-\frac{1}{2}} u_{n-1,m-1} \right\} + u_{n-1,m} + O(\Delta x, (\Delta\psi)^2) \quad (12)$$

$$T_{n,m} = \frac{\Delta x}{(\rho C_p)_{n-1,m}} \left(\frac{dp}{dx} \right)_n + \frac{\Delta x}{4(\Delta \psi)^2} \left(\frac{a}{C_p} \right)_{n-1,m} (u_{n-1,m+1} - u_{n,n-1})^2$$

$$+ \frac{\Delta x}{C_p \Delta \psi} \left[\left(\frac{C_p}{\sigma} a \right)_{n-1,m+\frac{1}{2}} T_{n-1,m+1} + \left(\frac{C_p}{\sigma} a \right)_{n-1,m+\frac{1}{2}} + \right. \quad (13)$$

$$\left. \left(\frac{C_p}{\sigma} a \right)_{n-1,m+\frac{1}{2}} \right] T_{n-1,m} + \left(\frac{C_p}{\sigma} a \right)_{n-1,m-\frac{1}{2}} T_{n-1,m-1} \left. \right\} + O(\Delta x, (\Delta \psi)^2)$$

where;

$$a \equiv \rho u (\rho \epsilon) \quad (14)$$

The linear algebraic Equations (12) and (13) are subject to a stability criterion which governs the permissible grid size. Based on the Von Neumann, stability analysis, (Reference (2)), which is strictly applicable to linear equations with constant coefficients, the criterion is:

$$\frac{\Delta \psi^2}{2a} > \Delta x < \frac{\sigma \Delta \psi^2}{2C_p a} \quad (15)$$

Finally, it is necessary to say a word about the form assumed for the eddy viscosity, $(\rho \epsilon)$, appearing in the coefficient a , Equation (14). For our purposes, following Reference (3), this has been taken as:

$$\rho \epsilon = K \delta^1 (u_e - u_o) \left(\frac{\rho_e^2}{\rho} \right) \left(\frac{\eta}{y} \right)^2 \quad (16)$$

where η is the transformed radial coordinate defined as:

$$\eta = \int_0^y \frac{\rho}{\rho_e} dy$$

δ^1 is the transformed jet radius, i.e., the value of η at which:

$$\frac{U_e - U}{U_e - U_0} = 0.01$$

and U_0 is the velocity on the jet centerline.

The above analysis has been programmed for digital computation on an I.B.M. 7094 digital computer.

III. CALCULATIONS

A set of calculations were performed to assess the effect of tangential mass injection as a means of obtaining the desired area change. The slot injection was approximated with the use of the above discussed jet mixing analysis; thus ignoring the effect of the shear at the wall. It is evident that the qualitative effect of the mixing is demonstrated by a jet analysis which does not require complex analytical and programming problems resulting from the no-slip condition on the wall. The jets were injected at subsonic Mach numbers into a field with an adverse pressure gradient. The static pressure of the jet was taken to be the same as that present in the main stream at the point of injection; hence, the stagnation pressure of the jet is much lower than that of the main stream.

As described earlier, based on purely inviscid considerations, this subsonic jet advancing in an adverse pressure field would decelerate and spread, with its cross-sectional area approaching infinity as the static pressure approached the stagnation pressure of the jet. The effect of mixing tends to counteract this; i.e., high velocity high stagnation pressure flow from the main stream, mixes in and energizes the jet stream, decreasing the cross-sectional area of the jet and allowing it to pass through high adverse pressure gradient fields. These two counteracting effects should enable the attainment of an arbitrary jet-spreading contour, for a given pressure gradient, by varying the Mach number and mass flow of the injected jet. Figure 6 shows, schematically, the separate effects of adverse pressure gradient, mixing, and the

combination of the two.

In addition, there exists the possibility of using a number of jets stationed at various downstream points as another controlling parameter. The additional jets would be used in the following way; suppose it were not possible to obtain enough of an area change from a single jet, as would occur if mixing energized the jet flow to such an extent that the streamline contour reached a peak and then began to decrease: then, at this point an additional subsonic jet would issue its low speed flow and the process would start all over again. In this manner multiple jets may be used to aid in overcoming the strong effects of turbulent mixing.

Figure 7 shows a sample calculation for a single jet in an arbitrary adverse pressure gradient field. The corresponding pressure distribution is shown in Figure 8. For this calculation the free stream Mach number has been chosen equal to 3; the jet Mach number equal to .45. Since the static pressure of the jet and main flow are equal and the stagnation to static pressure ratio of the jet is 1.15, the stagnation pressure of the jet is 273.5 p.s.f. The solid curve in Figure 7 represents the location of the streamline emanating from the lip of the splitter plate which initially separates the jet and the main flow. The contour formed by this streamline is equivalent to a body seen by the main stream. The dashed line represents the location of the same streamline if

the effects of viscous mixing are ignored; its location approaches infinity as the static pressure approaches the stagnation pressure of the jet.

The fact that the solid line in Figure 7 grows less steeply than the dashed line is due to the energizing of the jet flow by viscous mixing with the main stream. However, it is apparent that for the chosen pressure gradient the transfer of momentum between the two streams is not rapid enough to balance the inviscid spreading effect. To be sure no such streamline could exist in a supersonic stream; the flow would separate from the inlet wall with a resulting break-down of the boundary layer type flow.

The next calculation performed attempts to avoid this by decreasing the pressure gradient. The properties of the jet and main stream in this example are identical to those of Figure 7 and the streamline pattern is shown in Figure 9. Consider first regions I, II, and III of Figure 9. The pressure distribution is shown in Figure 10; it has been divided into linear segments for computational convenience. Dotted lines are drawn in Figure 9 to indicate that the apparent discontinuities of the streamlines are by no means physical in nature; they occur due to the discontinuous pressure distribution shown in Figure 10 and it is reasonable to assume that a smooth distribution would result with a smooth pressure variation. With this in view it appears that an appreciable area increase has been obtained utilizing a single slot. However, closer examination of this system from the point of view of asking if this is a physically stable flow is of importance. In Figure 11 there is plotted the velocity profiles at station D ($X = .13$ ft) of Figure 9. This

figure shows that the bulk of the jet is composed of flow with virtually zero momentum and any such flow will be subject to disturbances of a fluctuating nature and produce buzzing of the inlet similar to the phenomena found in circular inlets with vortical layers. To overcome this instability there has been positioned at station D an additional slot with the identical properties of the first slot. This is indicated on Figure 9 and once again the dotted line AB represents the displacement due to the slot; in practice this abrupt change would not occur since the slot would be buried in the wall. The curves labeled C and D represent the streamline location for the two different pressure distributions labeled in Figure 10. As can be seen the two pressure gradients differ by a very small amount and yet the streamlines exhibit entirely different behavior. Again examination of the velocity profile for curve C is enlightening. This is shown in Figure 12 and once again it is apparent that the majority of the jet has virtually no momentum and a situation of incipient separation exists. If the pressure gradient is lowered sufficiently to allow mixing to energize the jet, the area decreases rapidly as shown in curve D of Figure 9.

There are two conclusions to be drawn from this set of calculations. In the first place if any appreciable area increase is to be realized multiple slots must be used. In addition the new slot or slots must be introduced before the initial stream has lost so much of its momentum that instability occurs. Secondly, and this is an obvious point, the Mach number of the jet and main flow should be as close to each other as is reasonable; i.e. the difference in stagnation pressure of the two flows should be as small as possible.

With this in mind the next set of calculations was performed. In order to provide a more favorable set of conditions the main stream Mach number was reduced to 2 and the jet Mach number raised to .8. The slot injection scheme consisted of 4 slots shown schematically in Figure 13. The dashed line represents the desired contour which would result from the four slots located along the wall. An inlet, two feet in depth, was considered to be operating in a Mach number 2 airstream. It is desired to find a slot injection scheme whereby the necessary area reduction and pressure gradient in the inlet would be obtained. Assuming a Mach number of 1.2 at the inlet throat, the area reduction due to the jets should correspond to a depth of .6 feet and there should exist a static pressure ratio.

$$\frac{P_{\text{Throat}}}{P_e} = 3.0$$

The result of such a calculation is shown in Figure 14; the associated pressure gradient is shown in Figure 15. Again the apparent discontinuities in the dashed curve in Figure 14 arise from the physical displacement of the slot hardware which can, of course, be easily removed in any realistic design. The solid line shows the net effective area variation. It can be seen that the area decrease due to the jets is about 1.0 foot, while the pressure ratio is only 2.6 to 1. However, the physical height of the slots account for approximately .4 feet and if the slots are buried in the wall as suggested above, it would seem that the required area reduction has been obtained although the pressure ratio is slightly low.

In Figures 16, 17, 18 there are shown the velocity distributions at the axial location immediately before the three additional slots respectively. Although there is no way to analytically determine the optimum number of slots to use; i.e. to determine a lower bound on the slot momentum below which instability would occur, examination of Figures 16, 17, 18 would seem to indicate that the slot momentum has indeed been decreased significantly. Any further decrease of slot momentum; i.e. decreasing the number of slots or amount of mass flow out of the slots, should raise serious questions as to the stability of the flow.

Even though the desired area reduction is readily obtained by using the multiple slot injection scheme it is concluded from Figure 16, 17, 18, that it was necessary to use four slots. The resulting mass flow corresponds roughly to 20% of the capture mass in the typical inlet. Hence, for this scheme, the losses involved in capturing and slowing down this high amount of mass flow to subsonic velocities might be considered too extreme for practical use.

Since the point of view taken here is to design a system that would be of practical interest, the study of tangential injection was terminated. However, the basic premise of using mixing effects to control the contour of an inlet has been demonstrated as a valid one, and it is now believed that the drawback of the high mass flow rates necessary can be removed if the jets are issued at an angle to the main stream instead of tangential to it. In this way, inviscid interactions may be utilized. Such a study was initiated, making use of the same analytical model, and is reported in Part II of this report.

REFERENCES

1. Zeiberg, S.L., Bleich, Gary D., "Finite Difference Calculation of Hypersonic Wakes", AIAA Journal, Vol. 2, #8, August, 1964.
2. Richtmyer, R. D., "Difference Methods for Initial Value Problems", Interscience Publishers, N. Y., 1957.
3. Ting, L. and Libby, P., "Remarks on the Eddy Viscosity in Compressible Mixing Flows", Journal of the Aerospace Sciences, October, 1960.

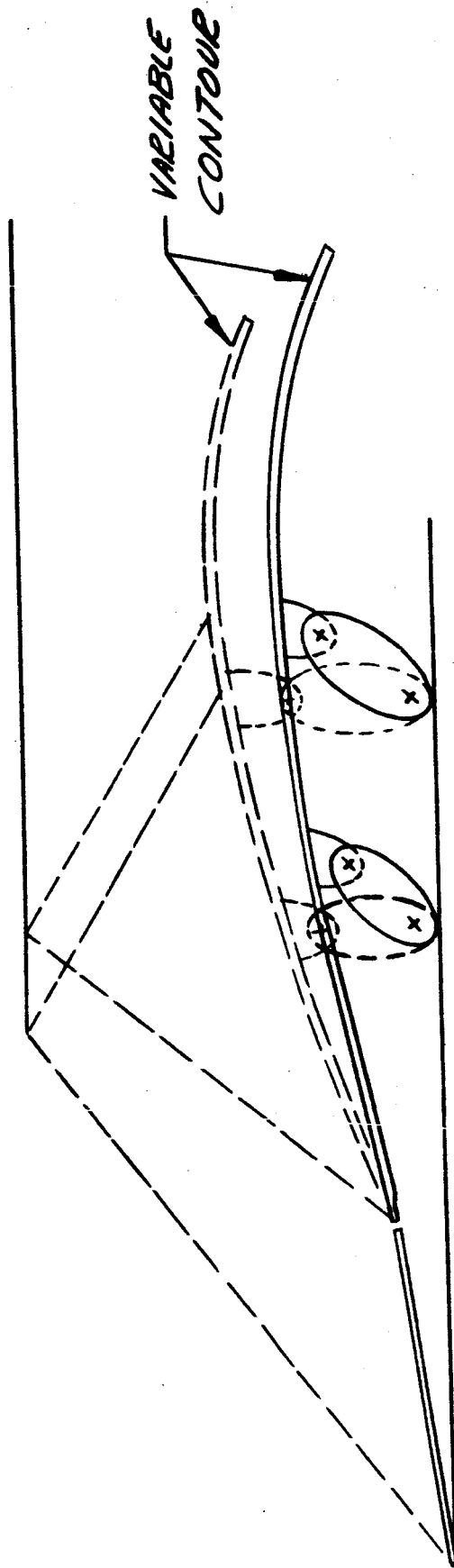


FIG. 1 SCHEMATIC OF MECHANICALLY CONTROLLED
VARIABLE CONTOUR INLET

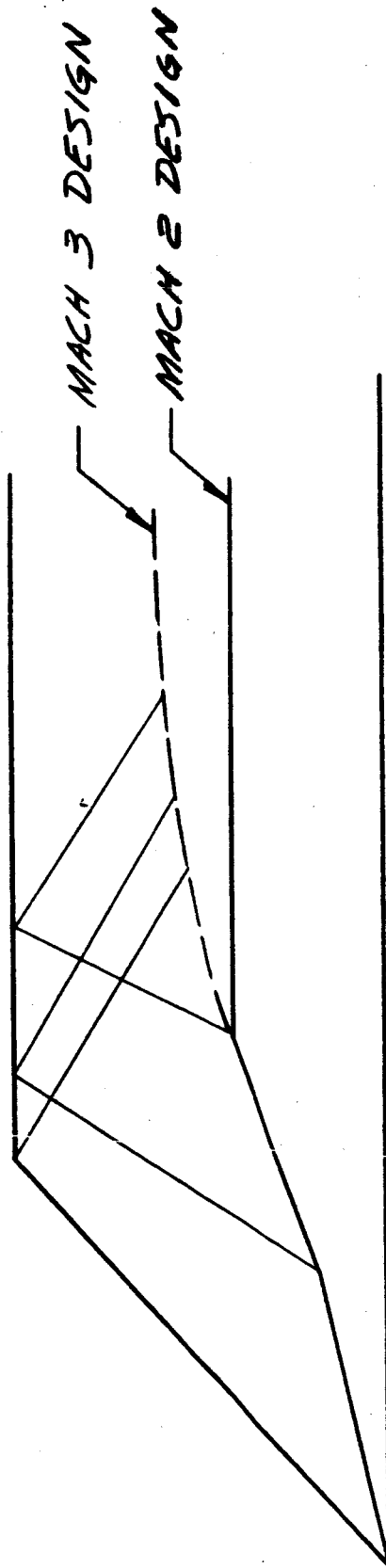


FIG 2 SCHEMATIC OF AREA CHANGE NECESSARY FOR
OFF-DESIGN OPERATION.

- ① ZERO MIXING
- ② MIXING EFFECT

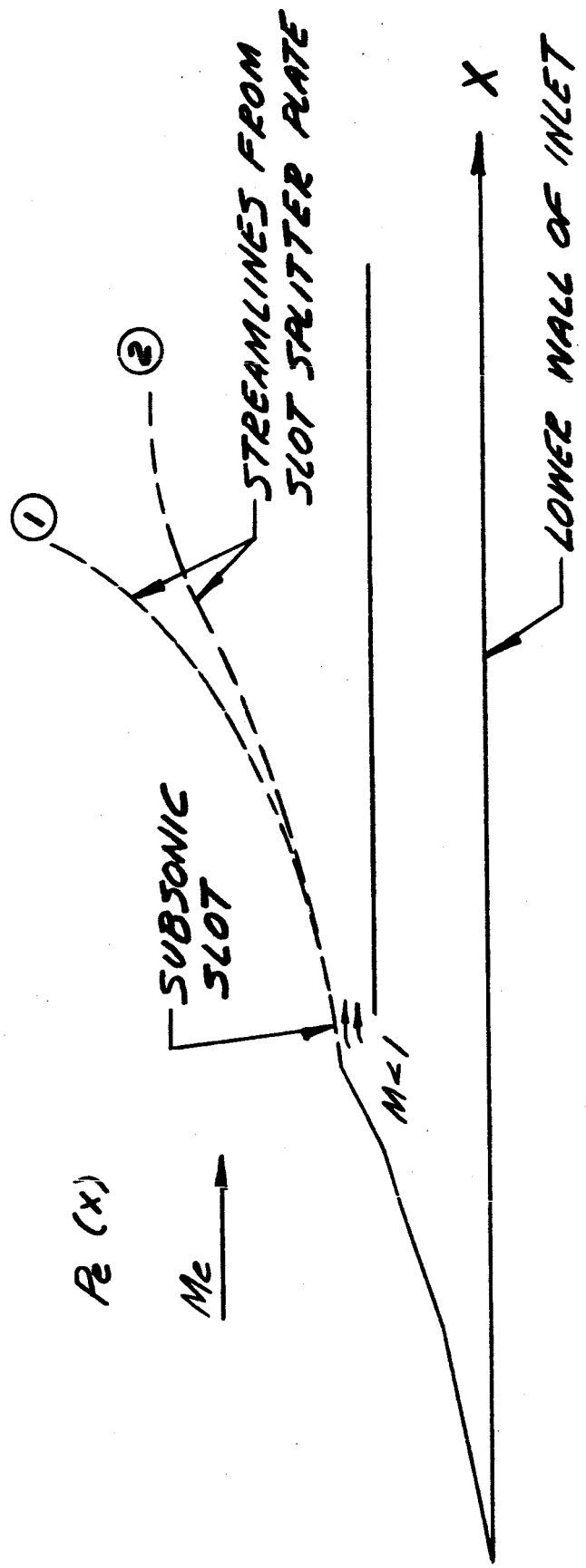


FIG 3 SCHEMATIC OF MIXING CONTROLLED CONTOUR

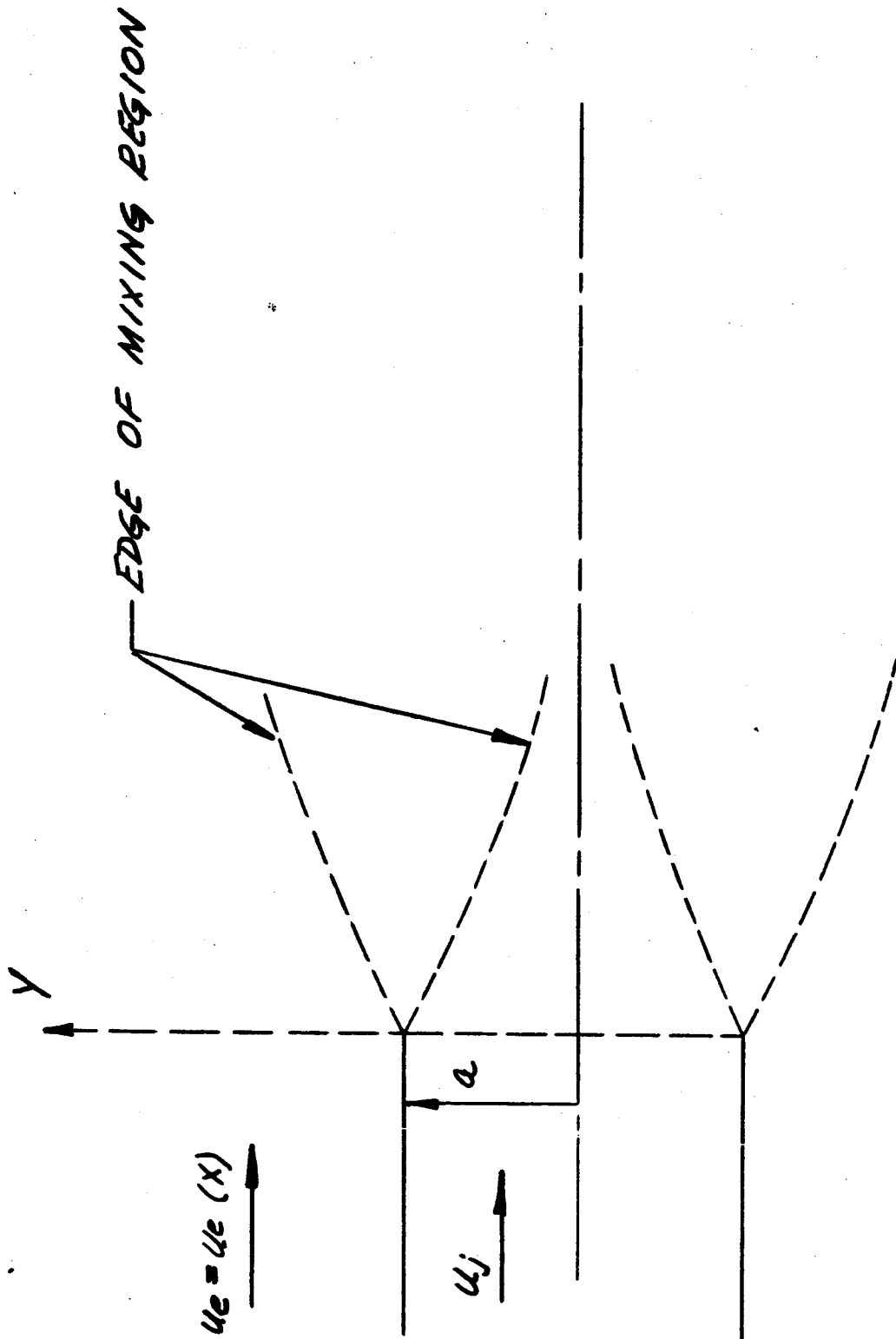


FIG. 4 SCHEMATIC OF TWO-DIMENSIONAL JET

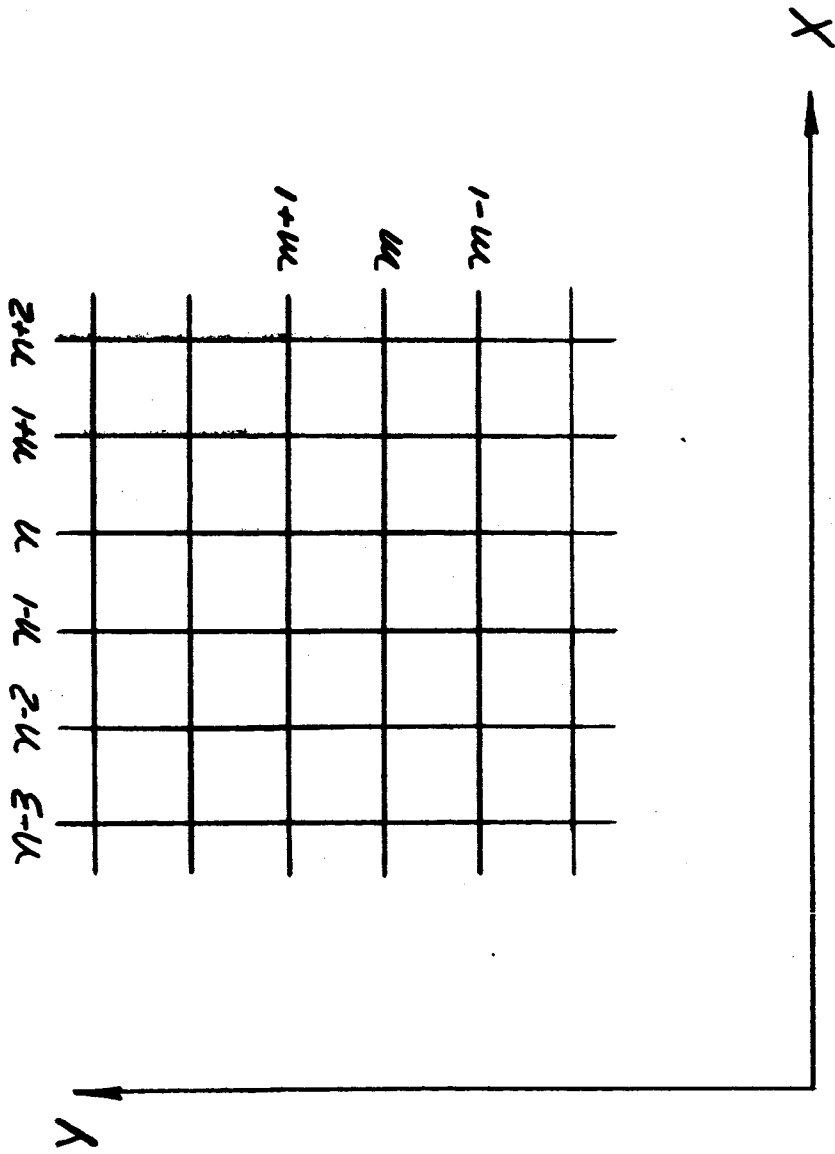


FIG 5 SCHEMATIC OF FINITE DIFFERENCE NETWORK

ZERO PRESSURE GRADIENT
STRONG ADVERSE PRESSURE GRADIENT
WEAK ADVERSE PRESSURE GRADIENT

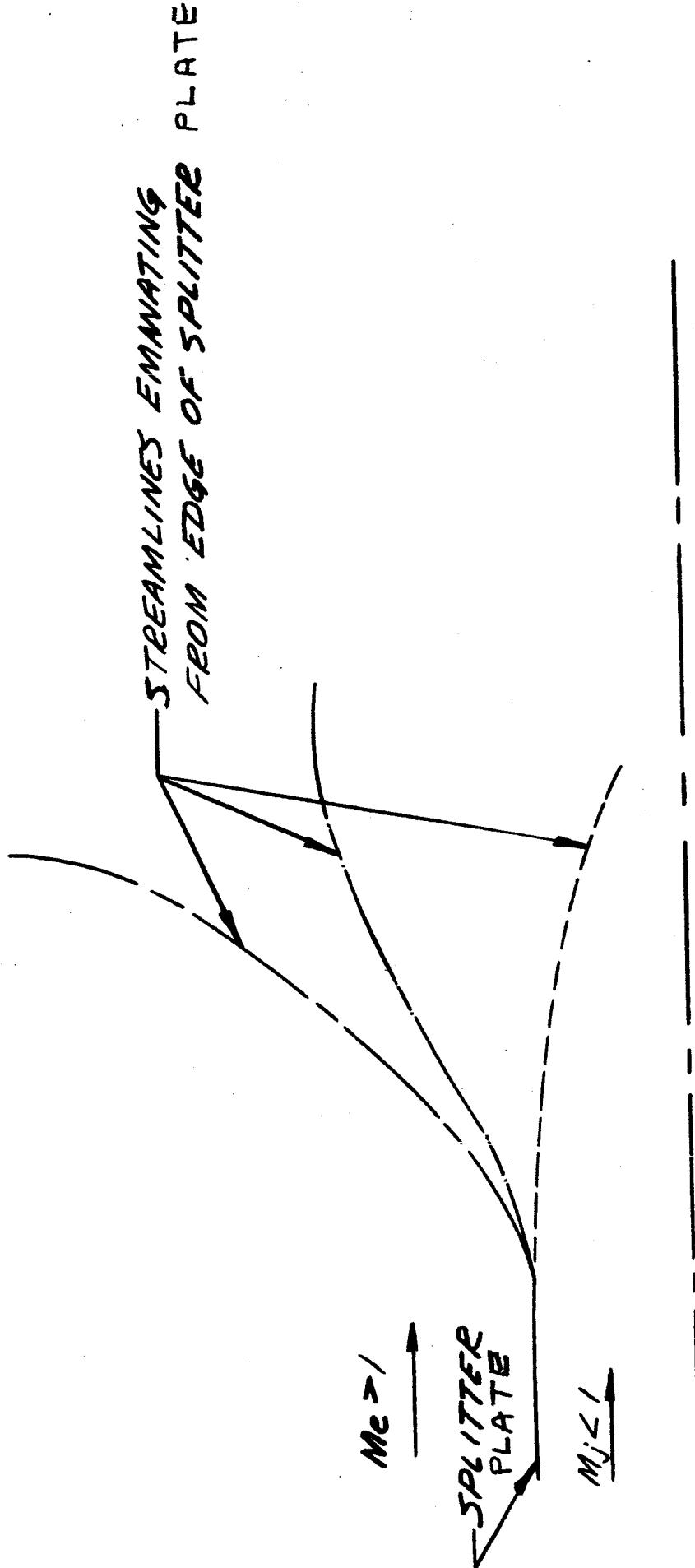


FIG 6 EFFECT OF PRESSURE AND MIXING ON CONTOURS FORMED BY JET SPREADING

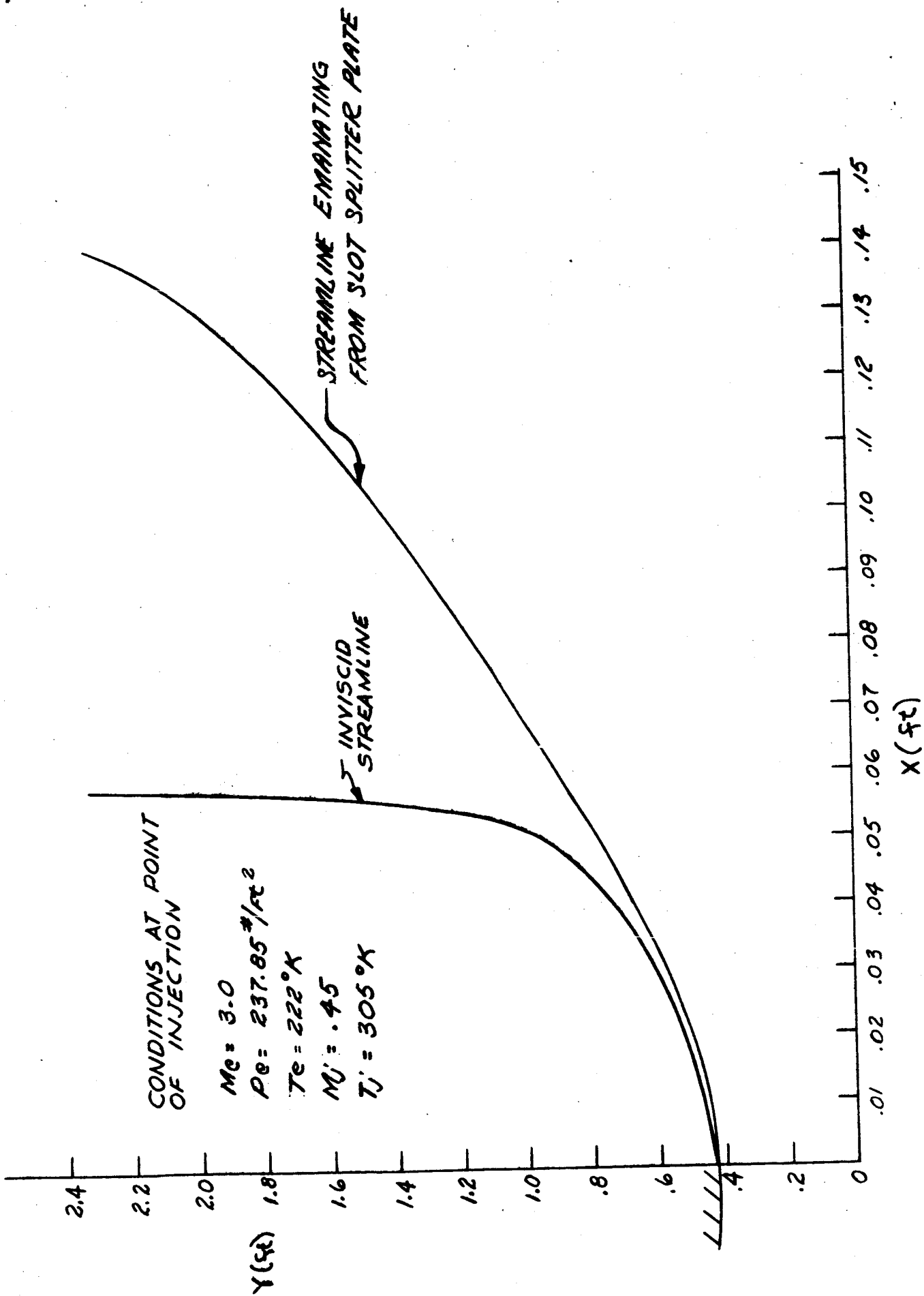


FIG. 7 CONTOUR FORMED BY SINGLE SLOT

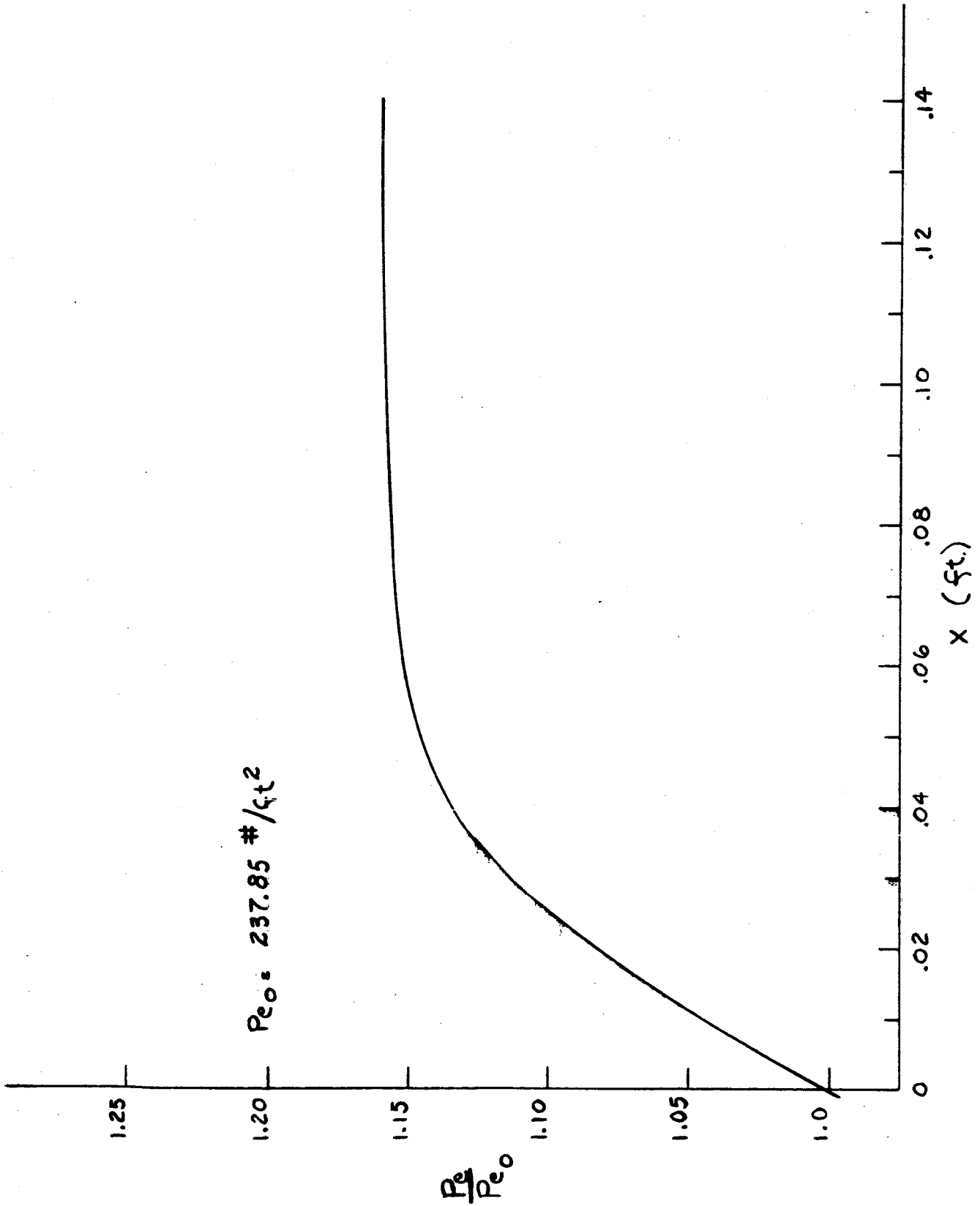


FIG. 8 PRESSURE GRADIENT FOR SINGLE SLOT

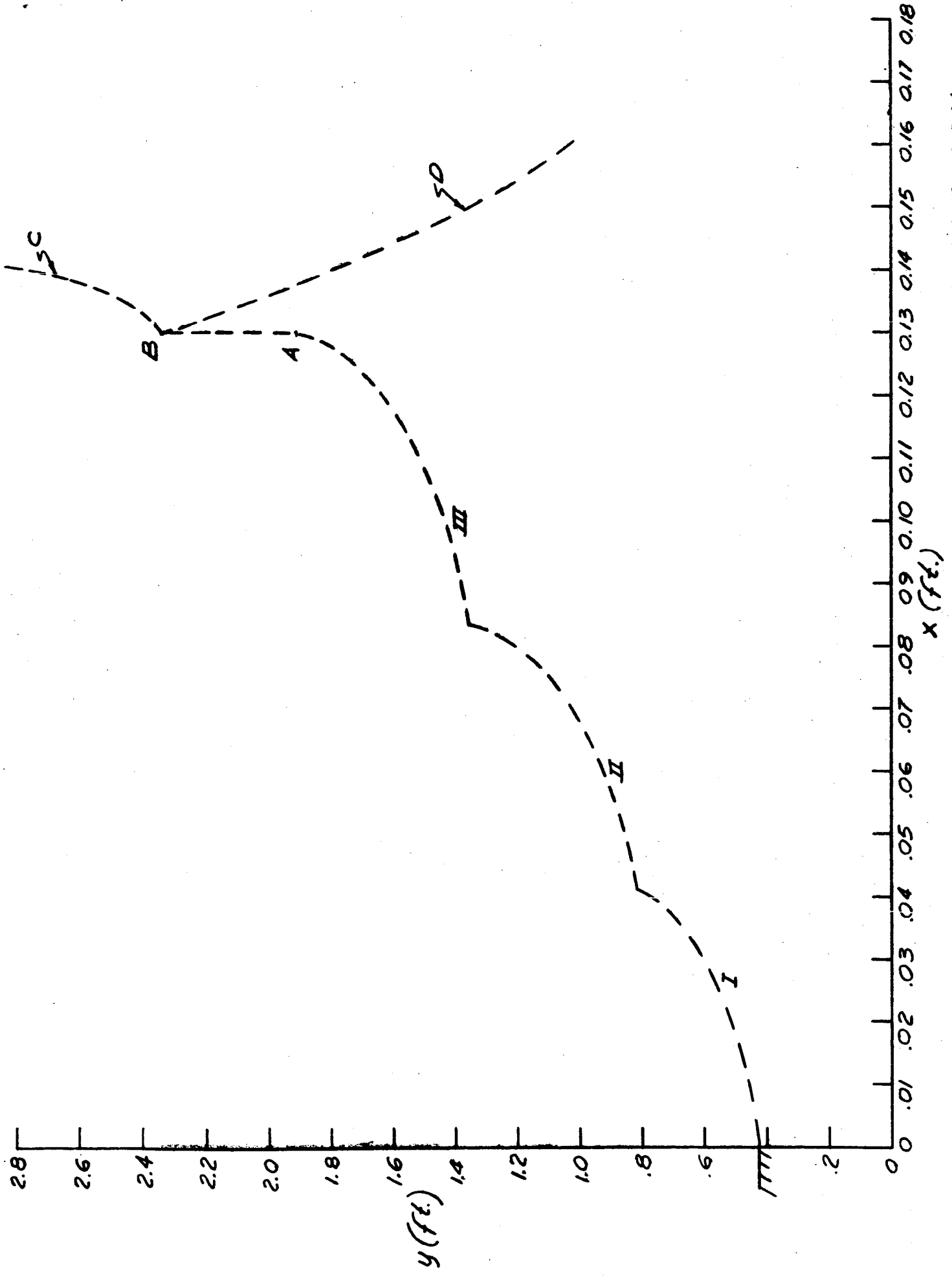


FIG. 9 CONTOUR FORMED BY SLOT INJECTION

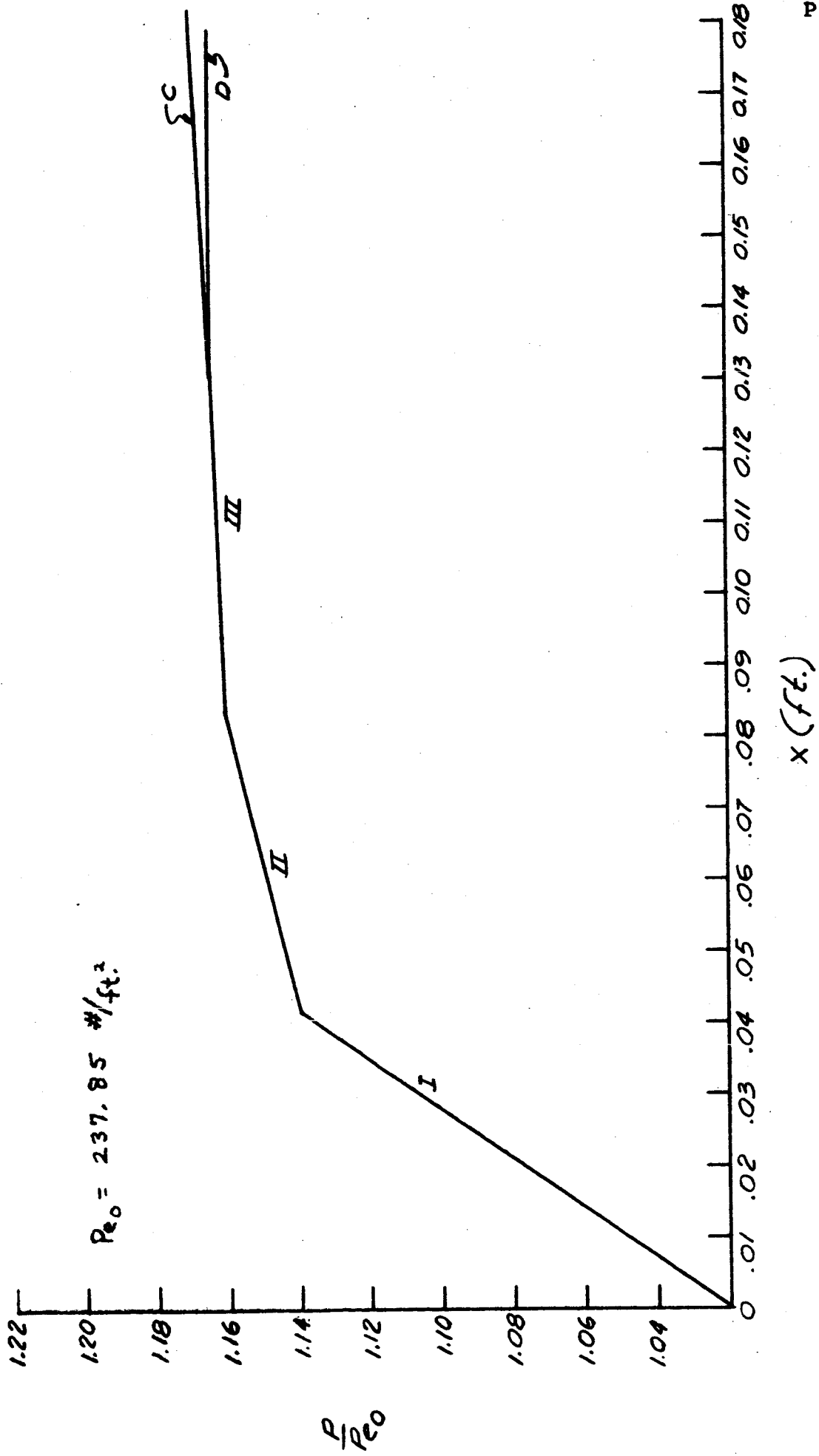


FIG. 10 PRESSURE GRADIENT

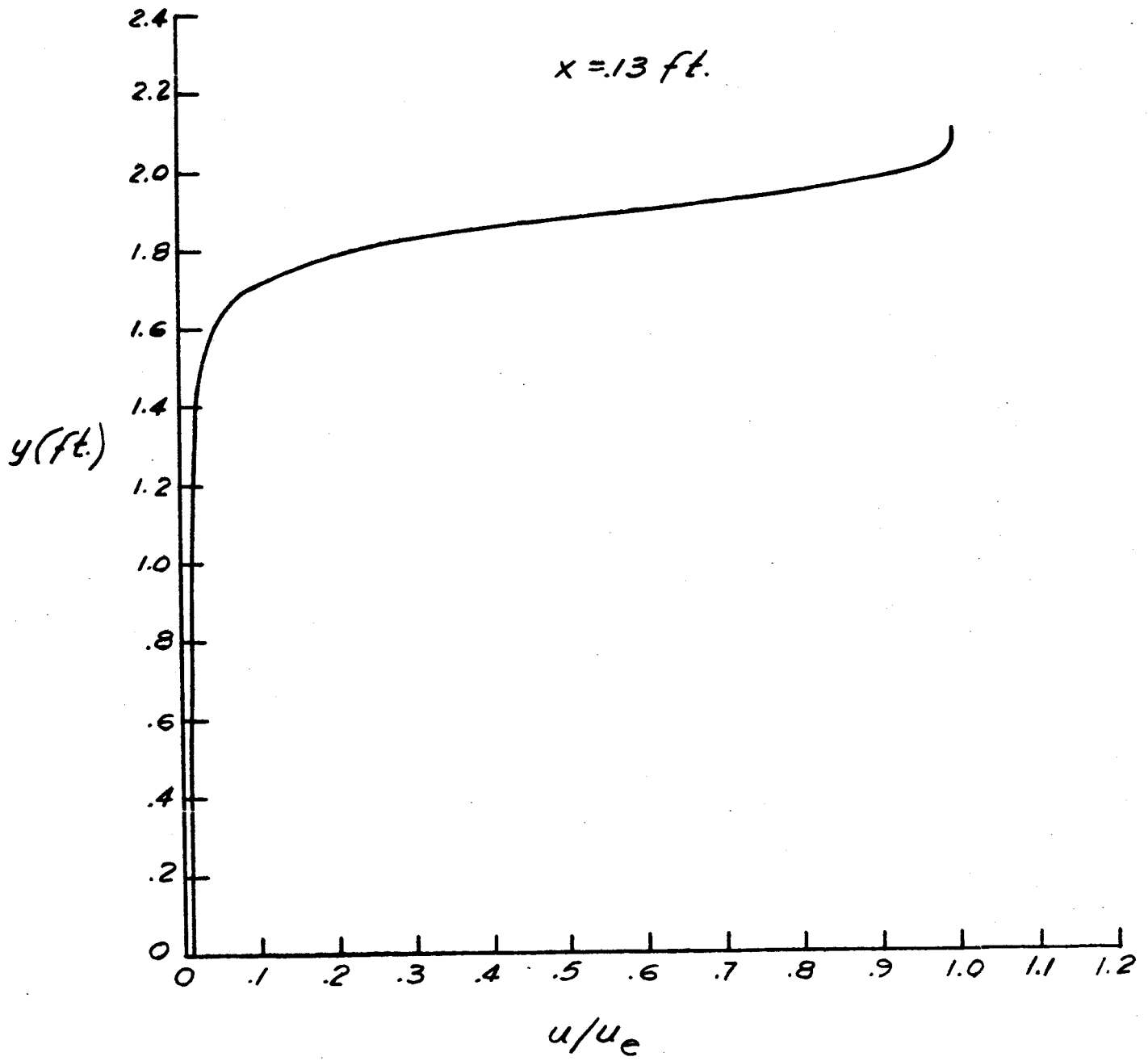


FIG. 11 VELOCITY DISTRIBUTION

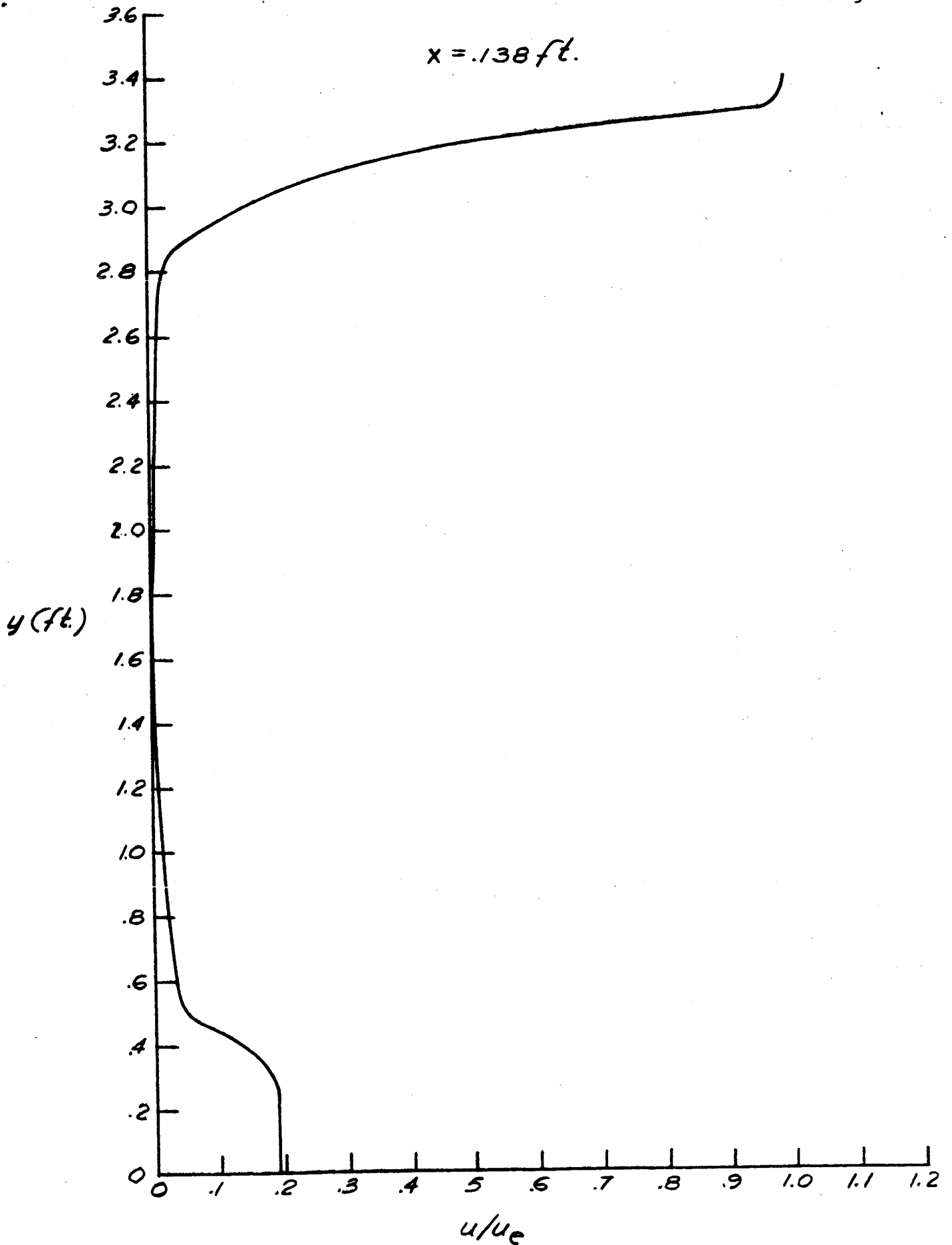


FIG. 12 VELOCITY DISTRIBUTION

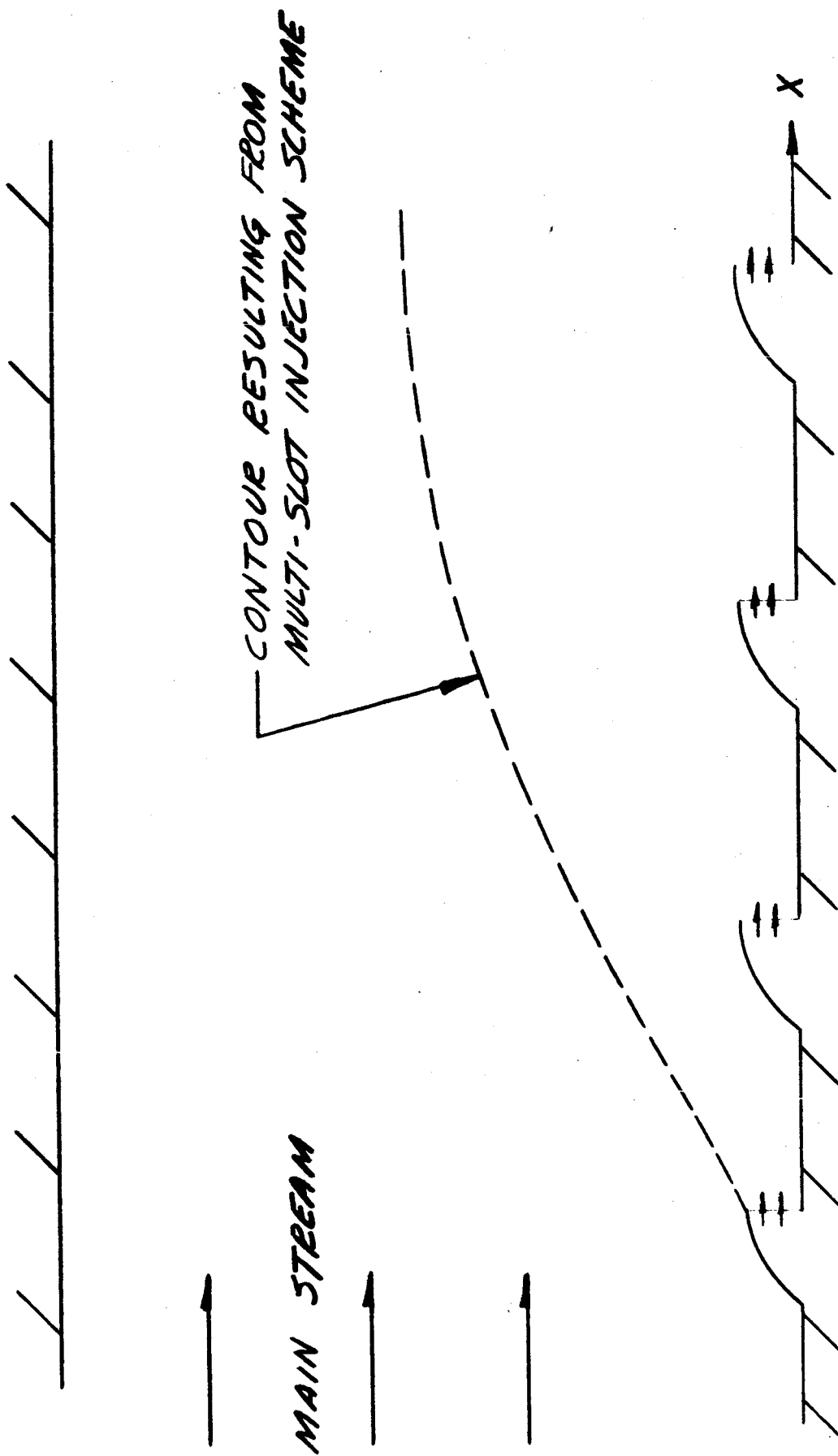


FIG 13 SCHEMATIC OF MULTI-SLOT INJECTION SCHEME

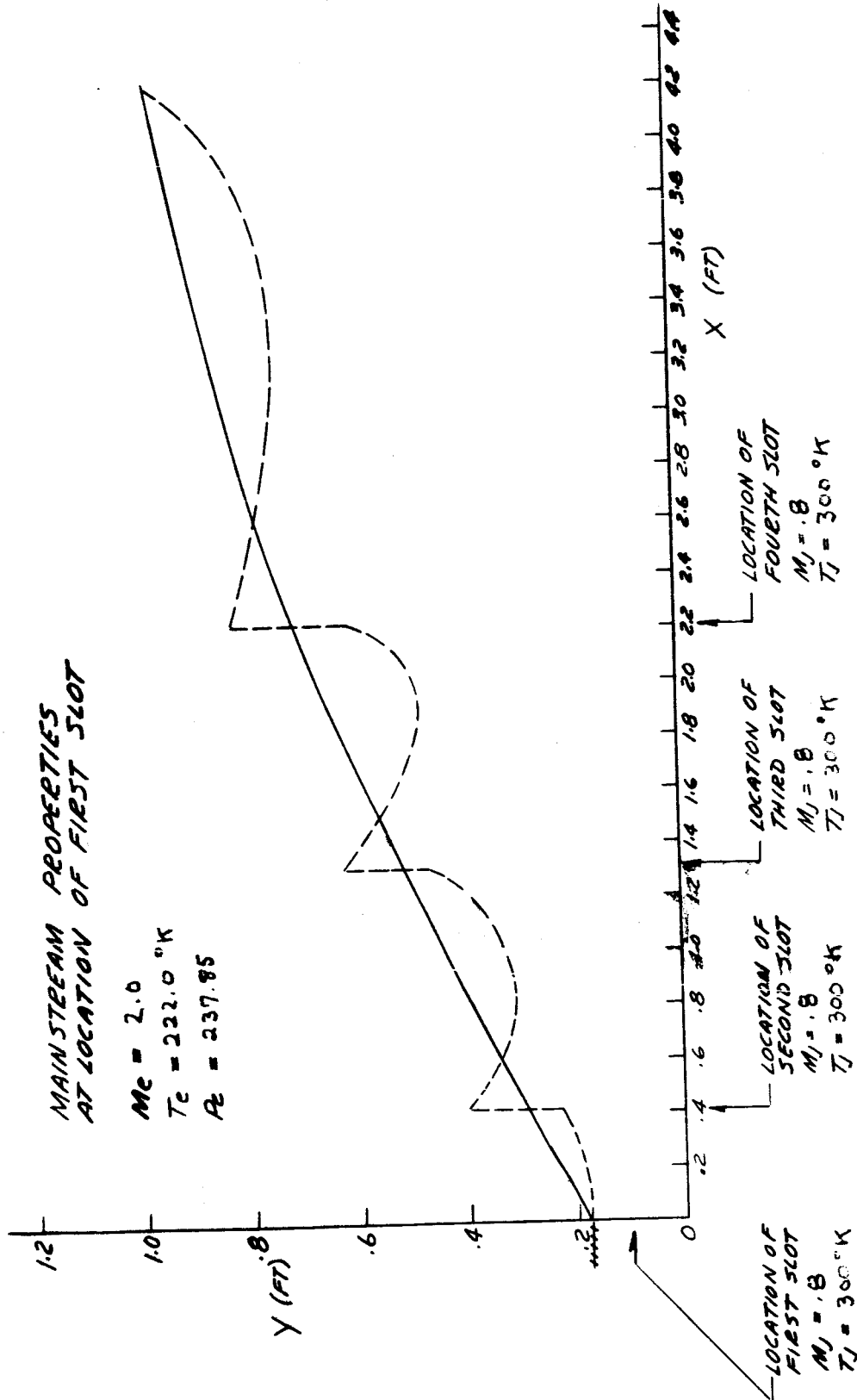


FIG 14 CONTOUR FOR MULTIPLE-SLOT INJECTION SCHEME

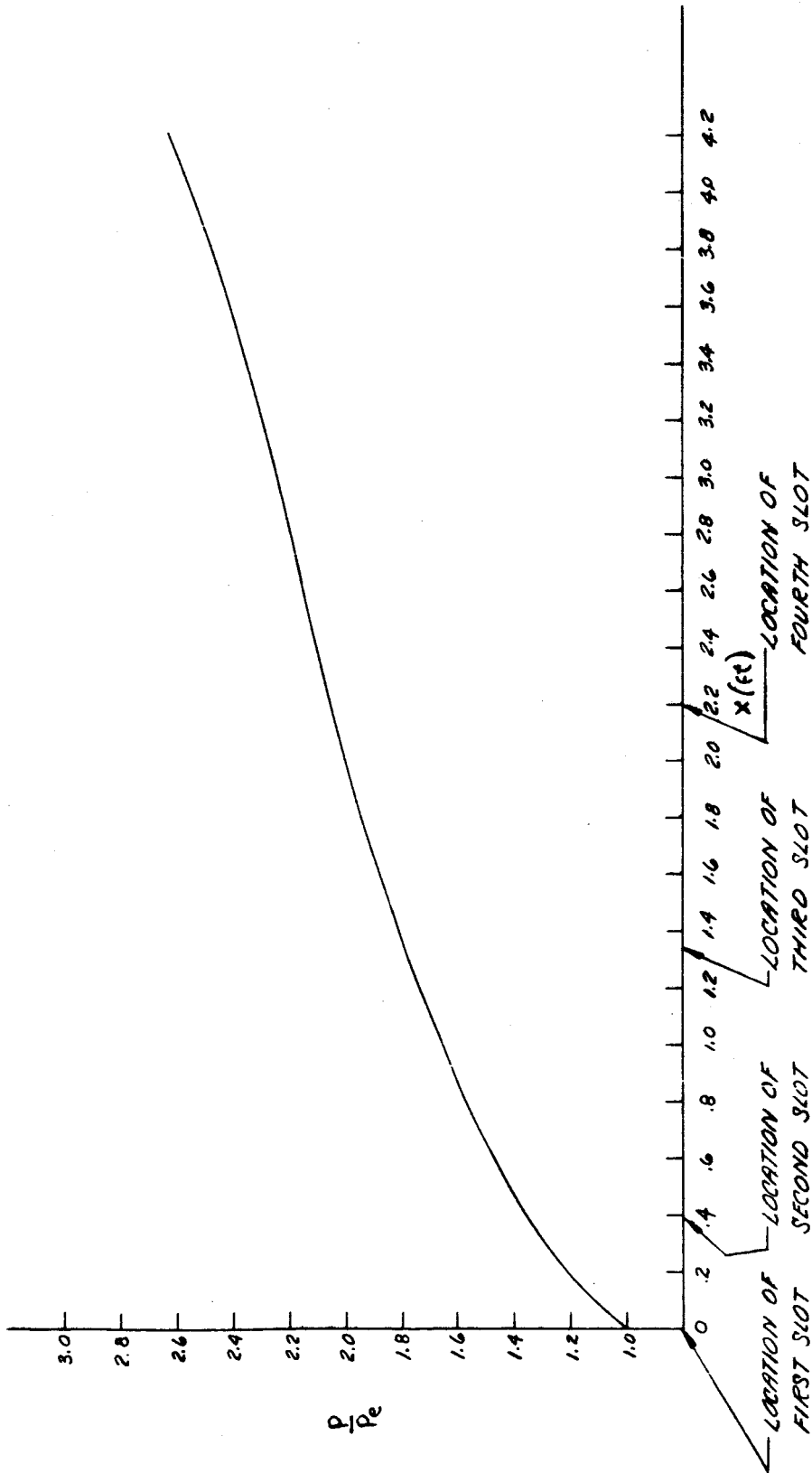


FIG. 15 PRESSURE DISTRIBUTION FOR MULTIPLE-SLOT INJECTION SCHEME

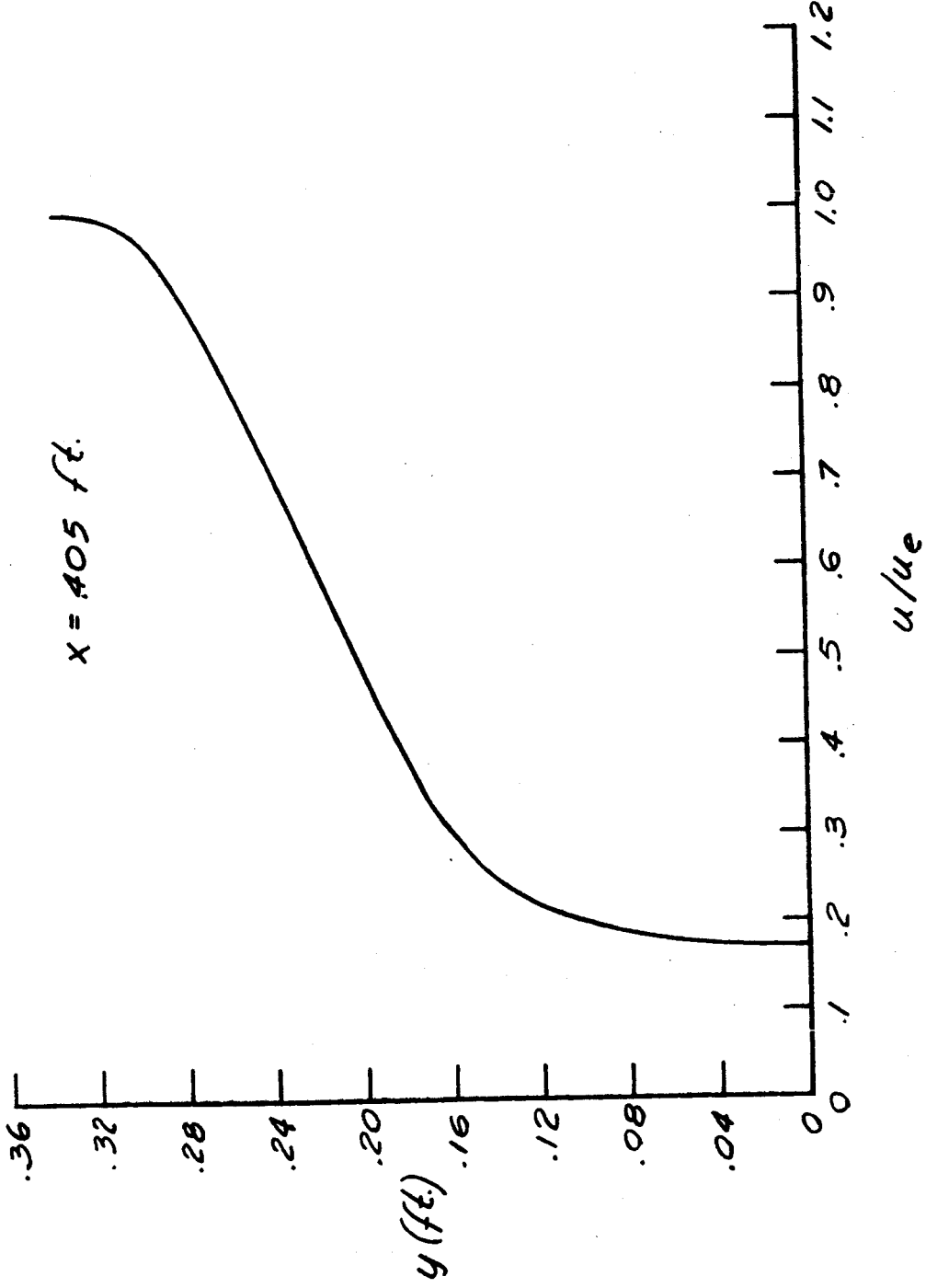


FIG. 16 VELOCITY PROFILE BEFORE SECOND SLOT INJECTION

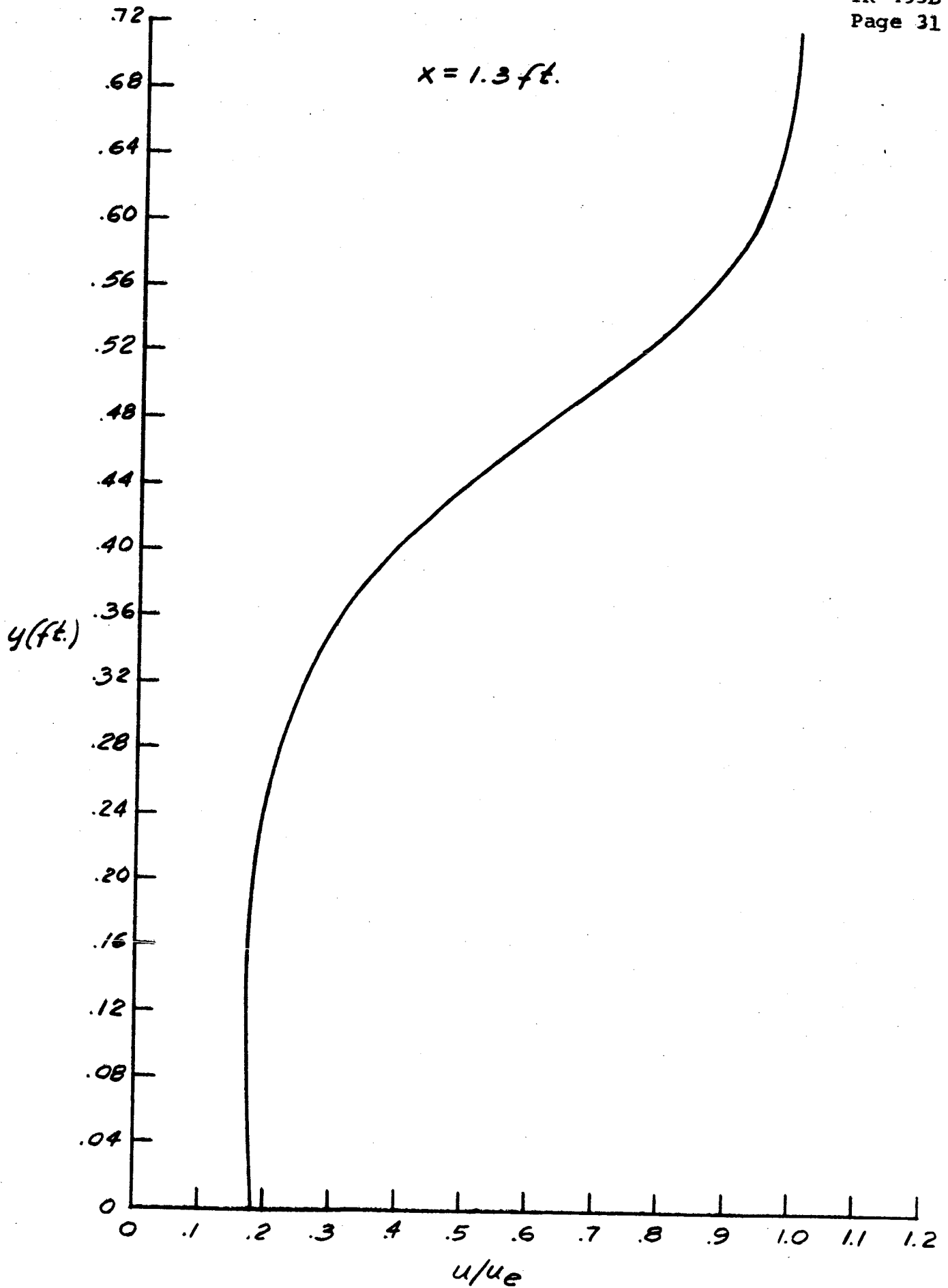


FIG. 17 VELOCITY PROFILE BEFORE THIRD SLOT

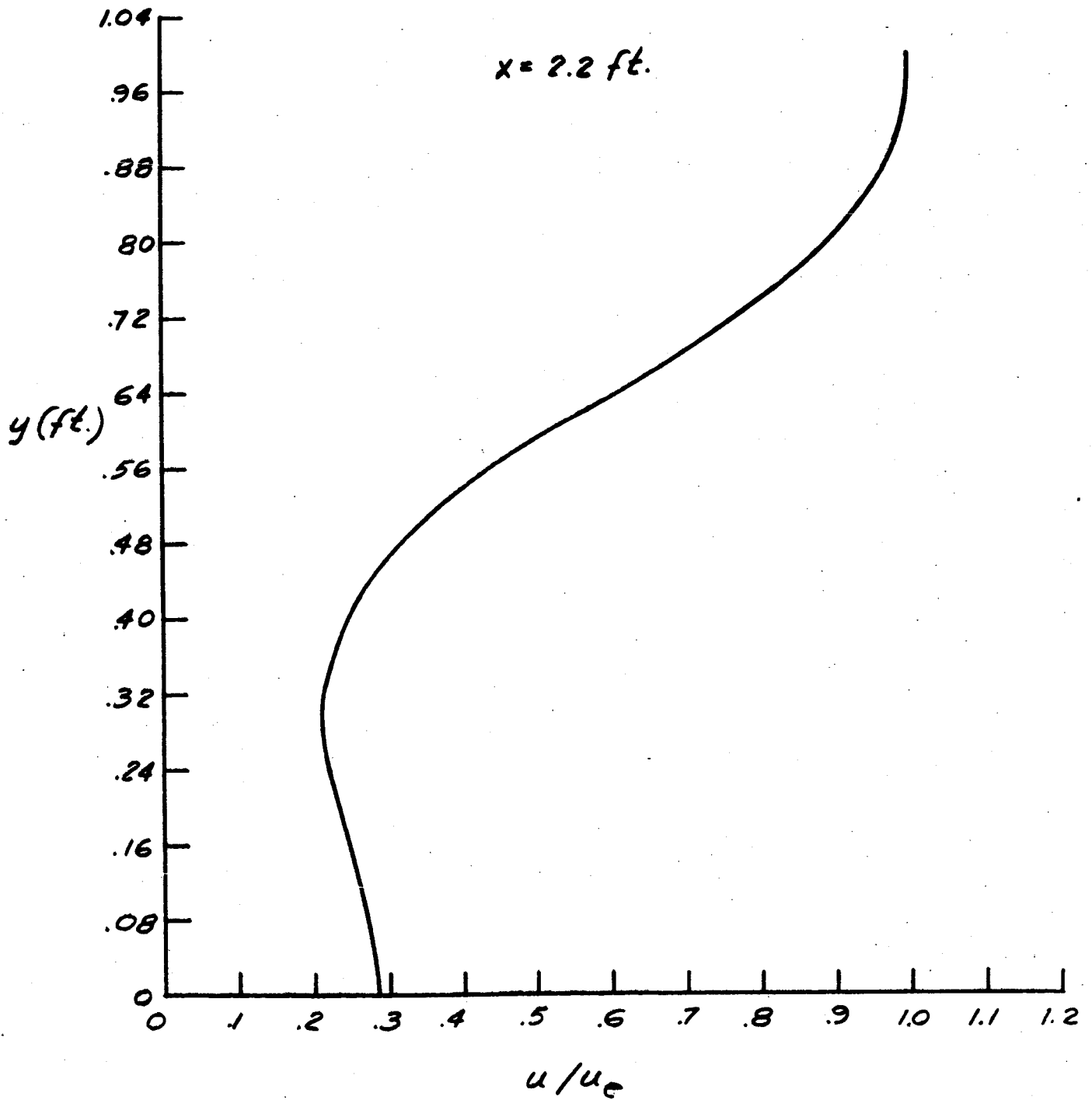


FIG. 18 VELOCITY BEFORE FOURTH SLOT INJECTION